Comparison of the Structural Performance of Monolithic and Precast Reinforced Concrete Core Walls*

Tadaharu NAKACHI[*1]

[*1] Department of Architecture and Environmental Engineering

In the core wall system in high-rise buildings, the four L-shaped core walls at the center effectively reduce seismic vibration. On the other hand, precast core walls are effective for construction because they can be built more quickly than cast-in-place core walls. In this study, a lateral loading test was conducted on a monolithic wall column simulating the corner and the area near the corner of an L-shaped core wall. The test results were compared with those of a precast wall column tested previously. The precast wall column was divided into precast columns, and horizontal tied rebars were concentrated at the second and third floor levels, and the mid height level of the first story. Based on a comparison of the results of lateral loading tests with monolithic and precast wall columns, the structural performance of these wall columns was clarified.

Key Words: Reinforced Concrete, Core Wall, Monolithic, Precast, Horizontal Tied Rebar, Cotter

1. Introduction

Multistory core walls installed in high-rise reinforced concrete buildings effectively reduce seismic vibration. On the other hand, precast core walls are effective for construction because they can be built more quickly than cast-in-place core walls. Regarding precast concrete multistory shear walls in high-rise buildings, Komiya et al. conducted lateral loading tests on wall columns having precast edge areas and examined their structural performance [(1)]. Kuboyama et al. also conducted lateral loading tests on core walls for which the edge areas were precast columns [(2)]. Previously, we conducted a lateral loading test on a full precast wall column simulating the area near the corner of an L-shaped core wall [(3)]. The specimen consisted of four square-section precast columns. The vertical joints between the precast columns were grouted with high-strength mortar. Each precast column had cotters at the vertical joint. Horizontal tied rebars were concentrated at the second and third floor levels to connect the precast columns. Furthermore, a lateral loading test was conducted on a wall column to which horizontal tied rebars were added at the mid height level of the first story[(4)], and the effect of horizontal tied rebars was clarified by comparing the results of both lateral loading tests[(5)]. In this study, a lateral loading test was conducted on a monolithic wall column corresponding to the precast wall column.

2. Summary of Test

2.1 Test Specimen

The configuration and arrangement of reinforcement in the specimen are shown in Fig. 1. The physical properties of the concrete and reinforcement are listed in Table 1 and Table 2, respectively. Two one-eighth-scale wall column specimens, Specimen PC0 and Specimen PC2, simulating the area near the corner of an L-shaped core wall were compared. Specimen PC0 was the monolithic specimen, and Specimen PC2 was the precast specimen tested previously[(4)]. Each specimen represented the lower three stories of a high-rise building of approximately 25 stories. The specimens had rectangular cross sections measuring 90 × 405 mm, were the flexural type and had a shear span ratio of

* 原稿受付　2014年2月28日
*1 建築生活環境学科
E-mail: nakachi@fukui-ut.ac.jp

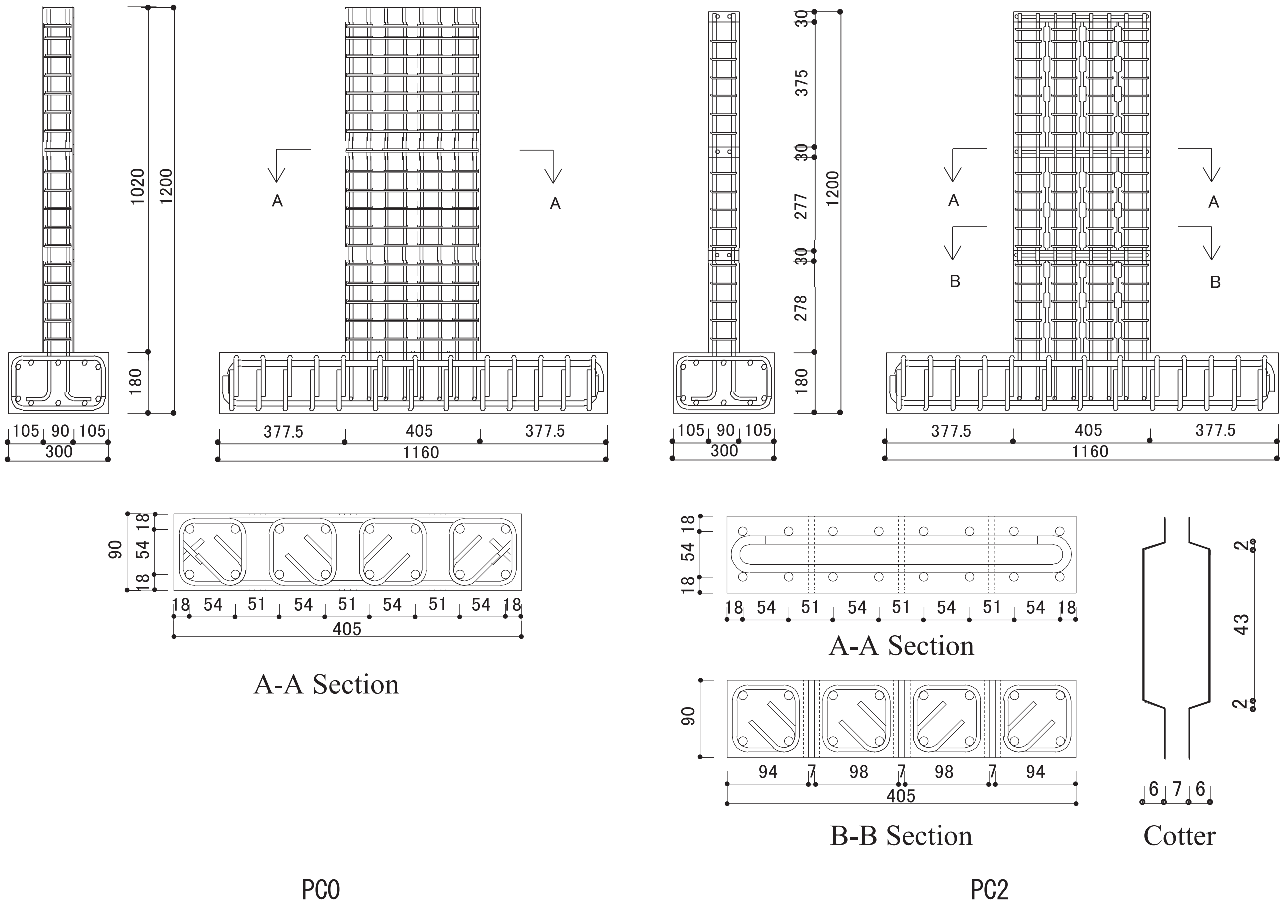

Fig. 1 Test Specimen

Table 1 Physical Properties of Concrete

Specimen		Compressive Strength (N/mm^2)	Young's Modulus (×10^{4}N/mm^2)	Sprit Strength (N/mm^2)
PC0		67.4	2.91	2.57
PC2	Precast	60.6	2.63	2.75
	Latter	58.7	2.65	2.13
	Grout	91.7	3.24	4.85

Table 2 Physical Properties of Steel

Bar Size	Yield Strength (N/mm^2)	Maximum Strength (N/mm^2)	Young's Modulus (×10^{5}N/mm^2)	Elogation (%)
D10	397	577	1.85	18.5
U5.1	1368	1491	2.11	9.3
D6	409	553	1.83	20.1

2.4. The specified design strength of the concrete was 60 N/mm^2. D10 deformation bars with yield strength of 397 N/mm^2 were used for the main bars and the horizontal tied rebars of Specimen PC2. High-strength U5.1 bars with a yield strength of 1368 N/mm^2 were used for the hoops. D6 deformation bars with a yield strength of 409 N/mm^2 were used for the transverse reinforcement of Specimen PC0. The pitch of the hoop and the transverse reinforcement was 55 mm. The specimen cover concrete was 6 mm thick.

The precast Specimen PC2 consisted of four square-section precast columns arranged in a line. The width of the opening between columns was 7 mm, and the openings were grouted. Each precast column had cotters without cotter bars at the vertical joint, and the depth of the cotter was 6 mm. The specified design strength of the grout was 80 N/mm^2. The concrete for the second and third floors was cast after the vertical joints of the precast columns were grouted. The horizontal tied rebars were concentrated at the floor level to connect the precast columns. Furthermore, the columns at the first story were divided into two parts at the mid height level of the first story and the concrete for the area between

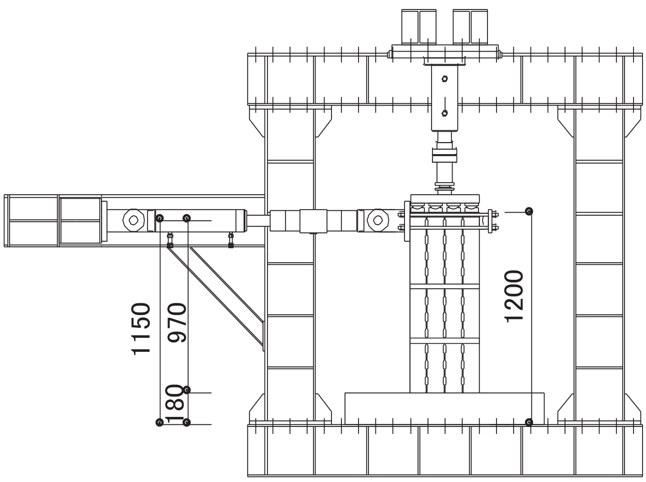

Fig. 2 Loading System

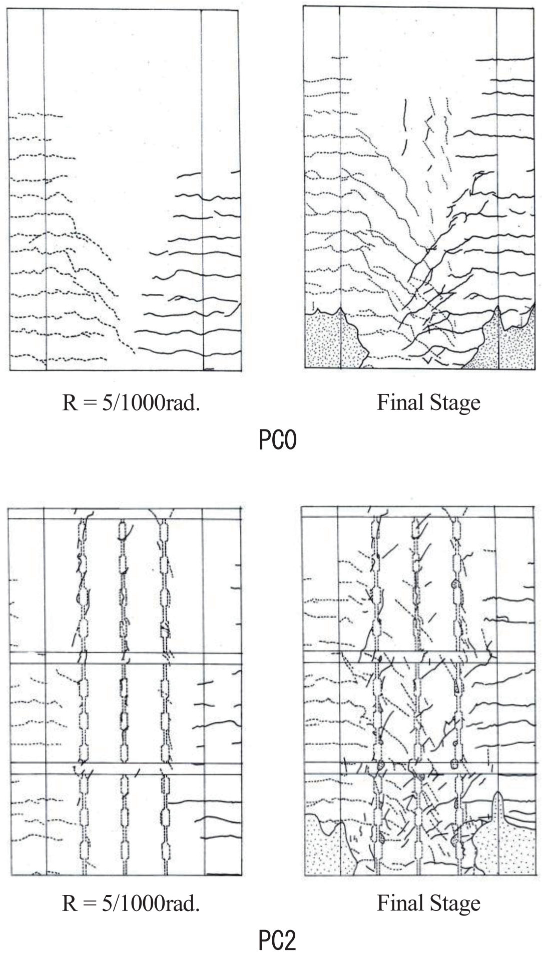

Fig. 3 Crack Patterns

the two parts was cast. The horizontal tied rebars were concentrated at the area between the two parts the same as at the second and third floor levels.

2.2 Test Procedure

The loading test was a cantilever type, as shown in Fig. 2. In the cyclic lateral loading test, the specimen was subjected to lateral forces by a horizontal hydraulic jack connected to the reaction frame. Positive loading was conducted by pulling the PC steel bars with the jack. The PC steel bars were attached to the pin support on the right side of the specimen (Fig. 2). Therefore, the specimen was pushed from the right side. Loading was conducted without tying the precast columns with the PC steel bars. Negative loading was conducted by pushing the specimen with the jack from the left side. A constant axial loading force was applied by a vertical hydraulic jack over the specimen to represent the axial stress in the stage of coupling beam yielding at the center core. The axial stress was 20% of the concrete compressive cylinder strength. The axial loads of Specimens PC0 and PC2 were 491 and 441 kN respectively. Loading was controlled by the horizontal drift angle at a height corresponding to the second floor level (h: 615 mm). The loading was cyclic lateral loading at R (drift angle) = 1/1000 (rad.) (1 cycle), 2/1000, 5/1000, 7.5/1000, 10/1000, 15/1000, 20/1000 (2 cycle respectively), 30/1000 (1 cycle). The relative displacement was measured by displacement transducers, such as the expansion and contraction of each segment and the relative sliding and opening displacement in the vertical joints. Strain gages were attached to the hoop, the horizontal tied rebars, the transverse reinforcement and the main bars. The attachment position of strain gages at the hoop was the midpoint of the side.

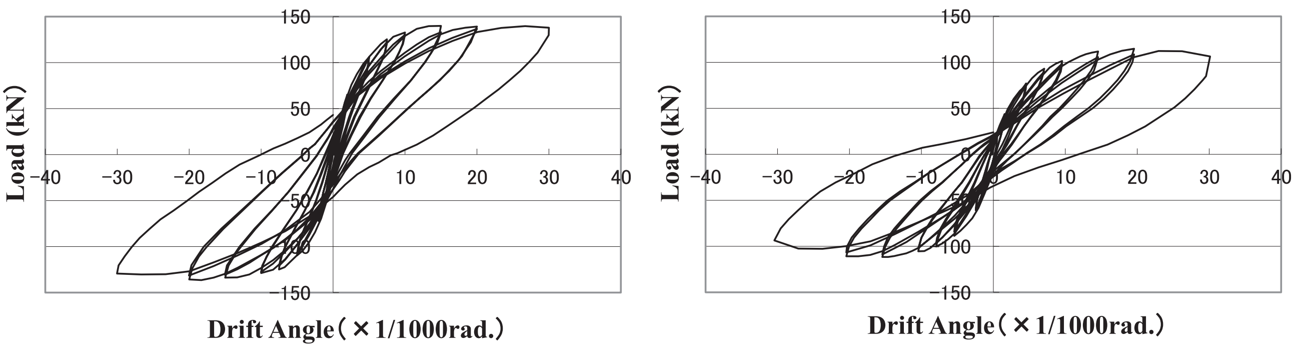

PC0 PC2

Fig. 4 Load - Deflection Curve

3. Test Results

3.1 Fracture Process

The crack patterns of the specimen at 5/1000 and the final stage are shown in Fig. 3. Under both positive and negative loadings, flexural cracks occurred by 2/1000 at the bottom of Specimen PC0. The flexural cracks then extended upward and to the middle of the specimen. After that, flexural shear cracks occurred by 5/1000. The corner area at the bottom appeared to crack vertically and crumbled slightly by 5/1000. After 7.5/1000, flexural cracks, flexural shear cracks and crumbling of concrete at the bottom expanded. With regard to the yield of reinforcement, the main bar at the compressive end yielded (yield strain 2146×10^{-6}) by 5/1000 under positive loading, and the main bar at the tensile end yielded by 7.5/1000. The specimen maintained the axial load by the final cycle at 30/1000.

Flexural cracks occurred by 2/1000 at the bottom of Specimen PC2 under both positive and negative loadings. The flexural cracks then extended upward and to the middle of the specimen. Shear cracks occurred at the cotter by 5/1000 and then extended. Under both positive and negative loadings, flexural shear cracks occurred by 5/1000. The corner area at the bottom appeared to crack vertically and crumbled slightly by 5/1000.

After 7.5/1000, extension of shear cracks at the cotter was not large, and flexural cracks, flexural shear cracks and crumbling of concrete at the bottom expanded. During the cycle of 30/1000, the strength decreased slightly, when a slight opening between the grout and concrete at the cotter was observed. With regard to the yield of reinforcement, the main bar at the compressive end yielded (yield strain 2146×10^{-6}) by 7.5/1000 under positive loading, and the main bar at the tensile end yielded by 15/1000. The specimen maintained the axial load by the final cycle at 30/1000.

3.2 Load–Deflection Curves

Figure 4 shows the load–deflection curves. The maximum strength of positive loading of Specimen PC0 was 139.8 kN at 15/1000, and that of negative loading was 136.5 kN at 20/1000. The strength decreased slightly during the last cycle of 30/1000 under negative loading. The maximum strength of positive loading of Specimen PC2 was 114.8 kN at 20/1000, and that of negative loading was 111.5 kN at 15/1000. The strength decreased slightly during the last cycle of 30/1000 under both positive and negative loadings.

3.3 Horizontal Distribution of Vertical Strain at the Bottom

Figure 5 shows the horizontal distribution of the vertical strain measured by displacement transducers. The measuring length was 65 mm. The figure shows the relationship between the vertical strain and the distance from the compressive end at the peak of positive loading for each drift angle. The strain of Specimen PC0 changed linearly from compressive to tensile between the compressive end and tensile end as a whole up to 30/1000. The strain of Specimen PC2 also

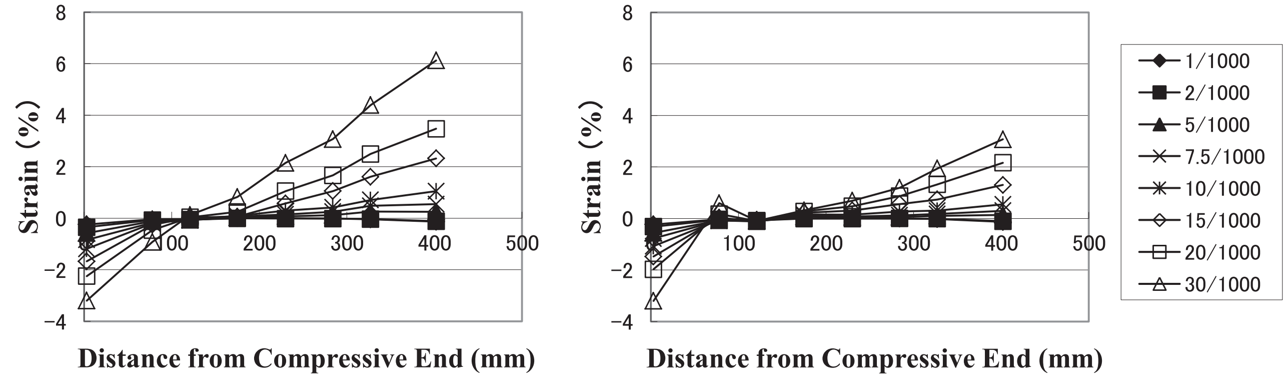

PC0 PC2

Fig. 5 Horizontal Distribution of Vertical Strain at Bottom

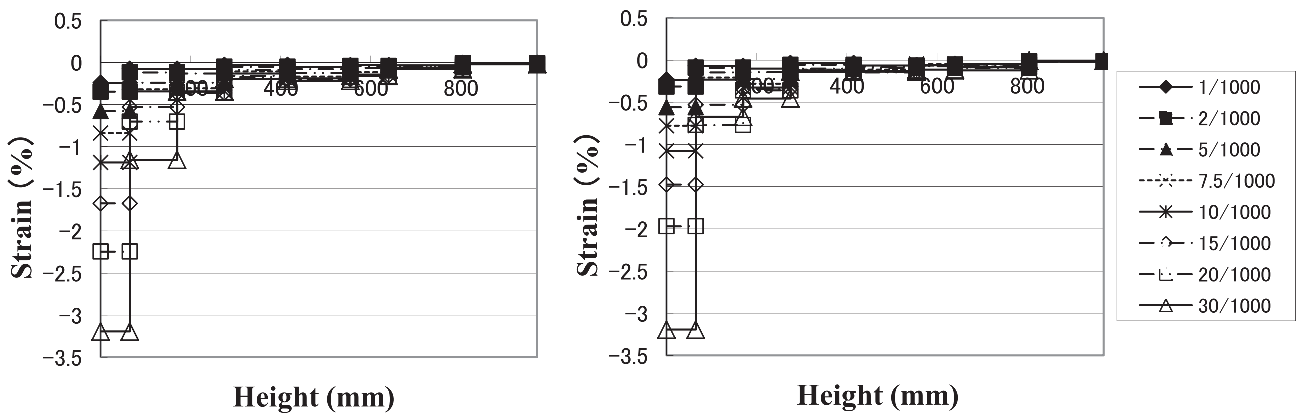

PC0 PC2

Fig. 6 Vertical Distribution of Strain at Compressive End

changed linearly from compressive to tensile as a whole up to 10/1000. The increase of tensile strain, especially at the tensile side, was smaller than that of Specimen PC0. On the other hand, the tensile strain at the point 78 mm from the compressive end increased after 20/1000. That is, independent movement was observed at the bottom of the precast column at the compressive end near the last stage.

3.4 Vertical Distribution of Strain at the Compressive End

Figure 6 shows the vertical distribution of the strain at the compressive end measured by displacement transducers. The figure shows the relationship between the vertical strain and the height from the bottom at the peak of positive loading for each drift angle. The strain of Specimen PC0 and Specimen PC2 increased with the increase in drift angle. The strain of both specimens was 0.5% at the bottom to the height of 65 mm at 5/1000, and 0.5% at the bottom to the height of 170 mm at 15/1000. The strain of Specimen PC0 at the height of 65 mm to 170 mm was larger than that of Specimen PC2 at 30/1000. The large strain area corresponded to the area where the concrete crumbled at the bottom mentioned above.

3.5 Horizontal Distribution of Strain of Main Bars at the Bottom

Figure 7 shows the horizontal distribution of the strain of the main bars at the height of 25 mm from the bottom. The figure shows the relationship between the vertical strain of the main bars and the distance from the compressive end at the peak of positive loading for each drift angle. The strain of Specimen PC0 and Specimen PC2 changed from

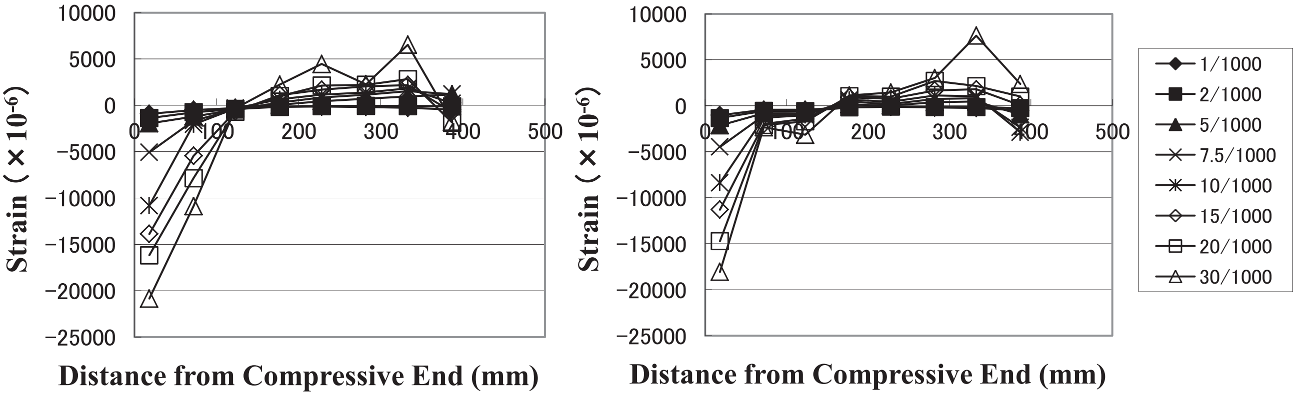

PC0 PC2

Fig. 7 Horizontal Distribution of Strain of Main Bars at Bottom

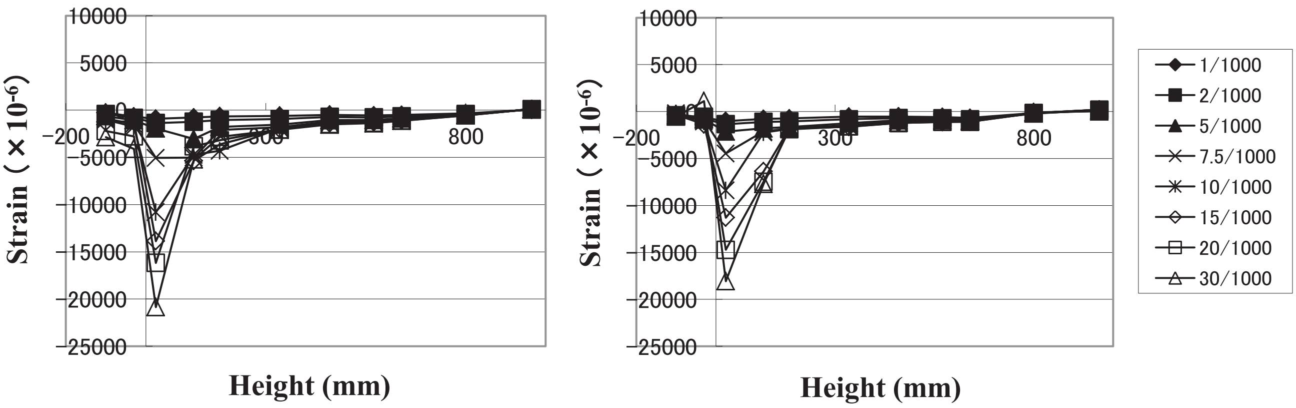

PC0 PC2

Fig. 8 Vertical Distribution of Strain of Main Bars at Compressive End

compressive to tensile between the compressive end and tensile end as a whole up to 30/1000 except for the tensile end. The strain at the compressive side of both specimens is larger than that of the tensile side. The strain at the point of 123 mm from the compressive end of Specimen PC0 hardly changed, so it is considered that this point is close to the neutral axis of the cross section. The strain at the point of 123 mm from the compressive end of Specimen PC2 was larger than that of Specimen PC0, and the strain at the point of 72 mm from the compressive end of Specimen PC2 was smaller than that of Specimen PC0. That is, independent movement was observed at the bottom of the precast column at the compressive end of Specimen PC2.

3.6 Vertical Distribution of Strain of Main Bars at the Compressive End

Figure 8 shows the vertical distribution of the strain of the main bars at the compressive end. The figure shows the relationship between the vertical strain of the main bars and the height from the bottom at the peak of positive loading for each drift angle. The strain of Specimen PC0 and Specimen PC2 increased with the increase in drift angle. The strain of both specimens increased near the bottom as a whole. Up to 5/1000, the strain of both specimens increased at an approximately constant rate toward the bottom. On the other hand, after 7.5/1000, the increment of strain near the bottom was remarkable. The area of remarkable increment was at heights below 185 mm of Specimen PC0, and below 120 mm of Specimen PC2 respectively. It is considered that this area corresponded to the area where the concrete crumbled at the bottom. The strain of Specimen PC0 at the height of 25 mm was larger than that of Specimen PC2 for each drift angle.

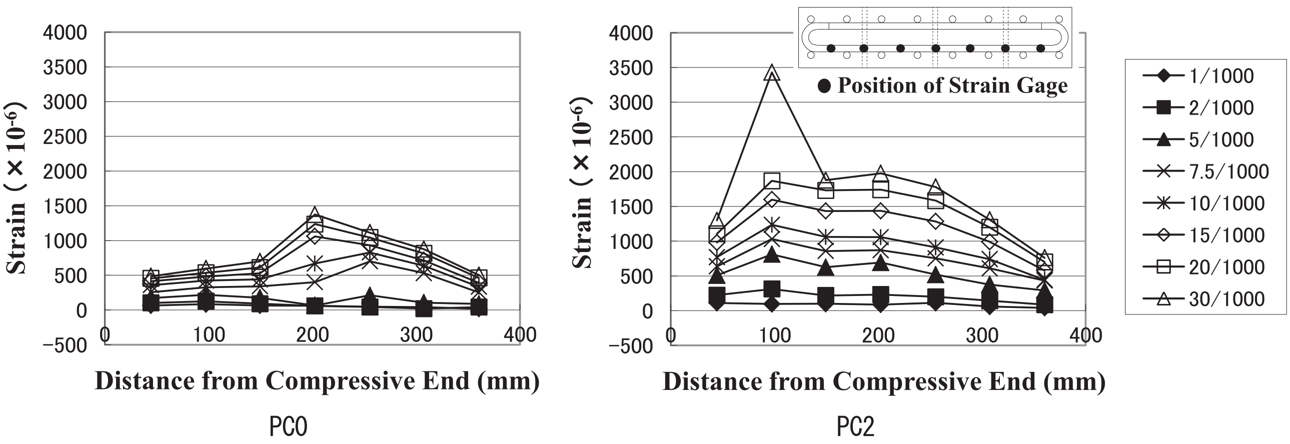

Fig. 9 Strain Distribution of Transverse Reinforcement and Horizontal Tied Rebars (Mid Height Level of First Story)

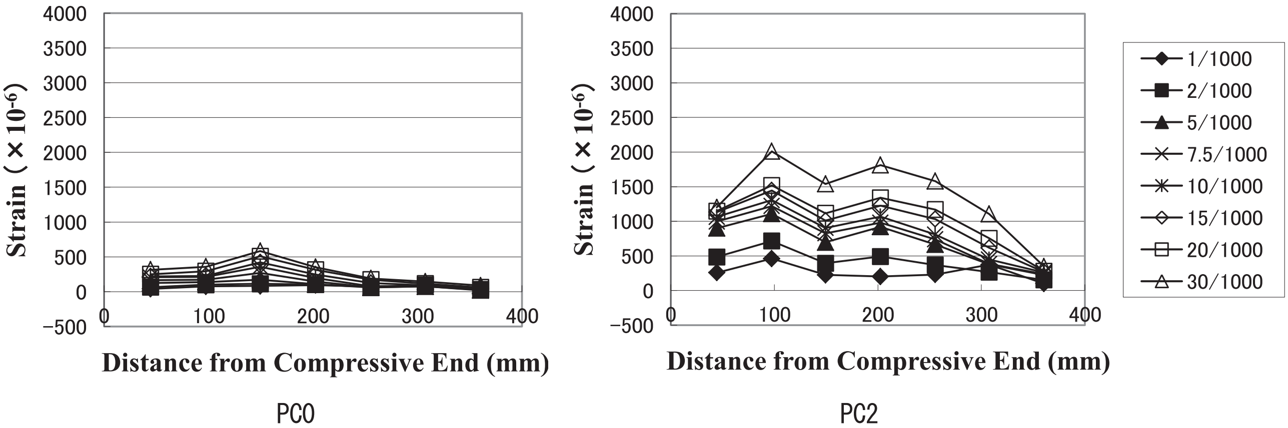

Fig. 10 Strain Distribution of Transverse Reinforcement and Horizontal Tied Rebars (Second Floor Level)

3.7 Strain Distribution of Transverse Reinforcement and Horizontal Tied Rebars

Figure 9 show the strain distribution of the transverse reinforcement of Specimen PC0 and the horizontal tied rebars of Specimen PC2 at the mid height level of the first story. The strain of both specimens increased with the increase in drift angle at all measuring points. The strain at the tensile end side of Specimen PC0 was larger than that at the compressive end side after 7.5/1000 as a whole. In the fracture process of Specimen PC0, flexural shear cracks occurred by 5/1000 and expanded after 7.5/1000 at the mid height level of the first story. Therefore, it is considered that the strain of the transverse reinforcement at the tensile end side increased due to flexural shear cracks after 7.5/1000. On the other hand, the strain at the compressive end side of Specimen PC2 was larger than that at the tensile end side as a whole. The strain at the point 93 mm from the compressive end, that is, the strain at the point on the boundary between the column at the compressive end and the next column, exceeded the yield strain and increased dramatically at 30/1000. On the load–deflection curves of Specimen PC2, the strength decreased slightly during the last cycle of 30/1000. It is considered that the reason for this decrease was a decline of unification and the independent movement of both these columns by yielding of the horizontal tied rebars at this boundary point.

Figure 10 shows the strain distribution of the transverse reinforcement of Specimen PC0 and the horizontal tied rebars of Specimen PC2 at heights corresponding to the second floor level. The strain of both specimens increased with the increase in drift angle at all measuring points. The strain at the compressive end side of both specimens was larger than that at the tensile end side as a whole. The strain at the point 93 mm from the compressive end of Specimen PC2 did not exceed the yield strain, unlike at the mid height level of the first story. The strain of Specimen PC0 was much smaller than that of Specimen PC2. It is considered that the reason for the small strain of Specimen PC0 was few cracks at heights corresponding to the second floor level.

4. Conclusions

A lateral loading test was conducted on a monolithic wall column simulating the corner and the area near the corner of the L-shaped core wall. The test results were compared with those of the precast wall column tested previously. Major findings are as follows.

(1) In the fracture process of the monolithic specimen, flexural cracks, flexural shear cracks and crumbling of concrete at the bottom occurred and expanded. The strength decreased slightly during the last cycle of 30/1000 under negative loading. On the other hand, in the precast specimen, shear cracks at the cotter and a slight opening between the grout and concrete at the cotter were also observed. The strength decreased slightly during the last cycle of 30/1000 under both positive and negative loadings.
(2) The vertical strain at the bottom of the monolithic specimen changed linearly from compressive to tensile between the compressive end and tensile end as a whole up to 30/1000. In the precast specimen, independent movement was observed at the bottom of the precast column at the compressive end near the last stage. That was observed by the horizontal distribution of the strain of the main bars at the height of 25 mm from the bottom, too.
(3) The vertical strain at the compressive end of the monolithic specimen at the height of 65 mm to 170 mm was larger than that of the precast specimen at 30/1000.
(4) A remarkable increment of the vertical strain of main bars at the compressive end was observed after 7.5/1000 at heights below 185 mm of the monolithic specimen, and below 120 mm of the precast specimen.
(5) It is considered that the strain of the transverse reinforcement of the monolithic specimen at the mid height level of the first story increased due to flexural shear cracks after 7.5/1000. On the other hand, it is considered that the decline of unification and the independent movement of the precast columns of the precast specimen were caused by yielding of the horizontal tied rebars at the mid height level of the first story.

Acknowledgement
This work was supported by JSPS KAKENHI (23560683).

References

(1) Y. Komiya, K. Yamamoto, et al., “Experimental study of R/C wall-columns with vertical joints between pre-cast and cast-in-place parts”, *Summaries of Technical Papers of Annual Meeting of Architectural Institute of Japan* (2003), pp. 255-258.
(2) H. Kuboyama, H.Nakazawa, et al., “Seismic behavior of precast R/C core walls of different strength”, *Summaries of Technical Papers of Annual Meeting of Architectural Institute of Japan* (2009), pp. 463-468.
(3) T. Nakachi, R. Tokunaga, “Experimental Study on Structural Performance of Precast Reinforced Concrete Core Walls (Part 1, Part 2) ”, *Summaries of Technical Papers of Annual Meeting of Architectural Institute of Japan* (2012), pp. 367-370.
(4) T. Nakachi, “Seismic Performance of Precast Reinforced Concrete Core Wall with Horizontal Tied Rebars at Mid Height Level of First Story” *Memories of Fukui University of Technology*, Vol.43(2013), pp. 181-190.
(5) T. Nakachi, “Effect of Horizontal Tied Rebars on Precast Reinforced Concrete Core Walls” *Memories of Fukui University of Technology*, Vol.43(2013), pp. 191-201.

（平成 26 年 3 月 31 日受理）